Journal of Hazardous Materials 213–214 (2012) 19–27

Contents lists available at SciVerse ScienceDirect

Journal of Hazardous Materials

journal homepage: www.elsevier.com/locate/jhazmat

Degradation of Malachite green by Potassium persulphate, its enhancement by 1,8-dimethyl-1,3,6,8,10,13-hexaazacyclotetradecane nickel(II) perchlorate complex, and removal of antibacterial activity

Subramanian Gokulakrishnan, Priyadarshini Parakh, Halan Prakash *

Department of Chemistry, Birla Institute of Technology and Science, Pilani, K.K. Birla Goa Campus, NH17B, Zuarinagar, Goa 403 726, India

ARTICLE INFO

Article history:
Received 23 April 2011
Received in revised form
31 December 2011
Accepted 10 January 2012
Available online 25 January 2012

Keywords:
Advanced oxidation process
Persulphate activation
Malachite green
Nickel(II) azamacrocyclic complex
Antibacterial activity

ABSTRACT

In this study, degradation of Malachite green (MG) (10 mg/L) by Potassium persulphate (KPS) (1 g/L), and KPS in presence of (1,8-dimethyl-1,3,6,8,10,13-hexaazacyclotetradecane) nickel(II) perchlorate (complex1), (200 μM), was investigated by spectrophotometric and HPLC methods. KPS alone had ability to degrade MG. Interestingly, rate of degradation of MG was enhanced upon addition of complex1. Degradation was effective at pH range of 3–9 and was found to be dependent on initial concentration of KPS, complex1, MG, and pH. Degradation of MG by KPS was not significantly affected in presence of Ni(II) ions whereas in presence of Fe(II) ions degradation was incomplete. Ability of KPS to reduce TOC increased in presence of complex1. Transformation products were analysed by LC–ESI–MS. Finally, treatment of MG with complex1 and KPS resulted in removal of antibacterial activity of MG under *in vitro* conditions.

1. Introduction

Malachite green (MG) is extensively used as a biocide in aquaculture, as colouring agent and additive in food industry, as disinfectant and antihelminthic in medical field, and also as dye in textile, paper and acrylic industries [1]. Despite its wide applications, use of MG has been banned in several countries and it is not approved by the US Food and Drug Administration [2] due to its harmful effects on immune system, reproductive system as well as its genotoxic and carcinogenic properties [3,4]. However, it is still being used in many parts of the world due to its low cost, ready availability and efficacy.

Moreover, MG is also environmentally persistent and poses potential environmental problems. MG has a strong absorption band in visible light region and when released in to water bodies could reduce transmission of solar light thereby affecting aquatic biota of the habitat. Thus, effective removal of MG from water bodies is environmentally very significant.

Conventional biological treatment processes [5,6], as well as biological decolourization of MG and related dyes using a batch and continuous system have been reported [7]. Microorganisms such as *Kocuria rosea*, *Cyathus bulleri* have been shown to degrade MG with efficiency more than 90%. However, these strategies were found to be time consuming, and require proper care for maintenance of microorganisms.

On the other hand, advanced oxidation processes (AOP's) are promising in development of treatment of wastewater, which are based on use of reactive oxidizing radicals that could rapidly degrade a variety of organic contaminants [8–12]. AOP's are not only less time consuming for effective degradation, they have added advantages like cost effectiveness, easy to treat, and usually do not produce toxic compounds during oxidation. Common oxidants used for AOP's include Permanganate, H_2O_2 (Fenton-like reactions), and Ozone [8].

Persulphate oxidation chemistry is an emerging technology in the field of AOP's to degrade organic contaminants [8,13,14]. Persulphate is relatively stable like permanganate. Moreover, it could be activated to generate reactive sulphate radicals and secondary radicals like OH•, similar to activation of H_2O_2 to produce radicals for degradation of a wide range of contaminants [13]. Thus, persulphate remains impressive because it offers advantages of both permanganate and H_2O_2 [13].

Thermal activation [14,15], UV-irradiation [14,15], base activation [16] and activation by transition metal catalysis [17] have been used to activate persulphate to generate reactive $SO_4^{\bullet -}$ radicals. Activation of persulphate by metal ion catalysis occurs by an

* Corresponding author. Tel.: +91 832 2580344; fax: +91 832 2557033.
E-mail addresses: halanprakash@bits-goa.ac.in, halanprakash@gmail.com (H. Prakash).
URL: http://universe.bits-pilani.ac.in/goa/halanprakash/Profile (H. Prakash).

0304-3894/$ – see front matter © 2012 Elsevier B.V. All rights reserved.
doi:10.1016/j.jhazmat.2012.01.031

oxidation – reduction reaction in which low valent metal ions M^{n+} act as electron donors (Reaction (1)) [14,15].

$$S_2O_8^{2-} + M^{n+} \rightarrow SO_4^{\bullet -} + SO_4^{2-} + M^{n+1} \quad (1)$$

Sulphate radicals produced during activation of persulphate initiates a cascade of reactions leading to formation of intermediate oxidants (H_2O_2, HSO_5^-) and reactive hydroxyl radicals, as shown in reactions (2)–(4), [18] which could effectively degrade a variety of organic contaminants.

$$SO_4^{\bullet -} + H_2O \rightleftharpoons HO^{\bullet} H^+ + SO_4^{2-} \quad (2)$$

$$SO_4^{\bullet -} + HO^{\bullet} \rightarrow HSO_5^- \quad (3)$$

$$2HO^{\bullet} \rightarrow H_2O_2 \quad (4)$$

Moreover, macrocyclic polyamine ligands such as tetra-, penta-, hexa-, azamacrocycles are extensively studied, and they generate continuous interest because of their biological properties and rich metal co-ordination chemistry [19,20]. A variety of azamacrocyclic complexes with nickel as metal ion are reported to exhibit different redox properties [21–24]. Earlier, Haines et al., has reported that persulphate could oxidize nickel tetra and penta azamacrocyclic complexes and this oxidation reaction occurs through an ion-pair mechanism leading to generation of reactive sulphate radicals and stable trivalent nickel species (reactions (5) and (6)) [25]. Moreover, trivalent nickel species are also known to act as strong oxidants [26].

$$[Ni(II)L]^{2+} + S_2O_8^{2-} \underset{\text{ion-pair}}{\{Ni(II)L^{2+}, \quad S_2O_8^{2-}\}} \quad (5)$$

$$\{Ni(II)L^{2+}, S_2O_8^{2-}\} \rightarrow [Ni(II)L]^{3+} + SO_4^{\bullet -} + SO_4^{2-} \quad (6)$$

L, Azamacrocyclic ligand.

Based on above facts, we envisaged that persulphate, and persulphate in presence of nickel azamacrocyclic complex could be useful for degradation of MG. AOP's such as Ozonation [27], Photocatalyst assisted degradation [28,29] Fenton processes [30], Photodegradation by UV/H_2O_2 [31] and Microwave assisted photocatalytic degradation [32] have been explored for degradation of MG, emphasizing the need of alternative methods for degradation of MG. However, activation of persulphate by nickel azamacrocyclic complex and its effect on MG has not been studied.

Present report is focused on study of effect of (i) Potassium persulphate (KPS) oxidation, (ii) (1,8-dimethyl-1,3,6,8,10,13-hexaazacyclotetradecane) nickel(II) perchlorate (complex1), (Fig. 1) and KPS oxidation system and (iii) Transition metal ions [Ni(II)/Fe(II)] and KPS oxidation system on degradation of MG by spectrophotometric as well as high pressure liquid chromatographic (HPLC) methods. The effect of various parameters such as initial oxidant concentration, catalyst concentration, dye concentration and pH was studied. We also examined antibacterial activity of MG after its degradation by KPS and complex1 oxidation system. Change in total organic carbon (TOC) was analysed. Degradation intermediates were identified by liquid chromatography electrospray ionization mass spectrometry (LC–ESI–MS), and possible degradation pathway was proposed.

2. Materials and methods

2.1. Reagents

$NiCl_2{\cdot}6H_2O$, $FeSO_4{\cdot}7H_2O$, $K_2S_2O_8$, H_2SO_4, NaOH of guaranteed analytical grade from SD fine chemicals, India were used. Malachite green (MG) was obtained from Hi media, India. Complex1 was prepared and purified according to earlier report [33]. Care must be taken as large amount of perchlorate salts could be explosive [33]. For HPLC analysis, acetonitrile (HPLC grade) and Millipore water

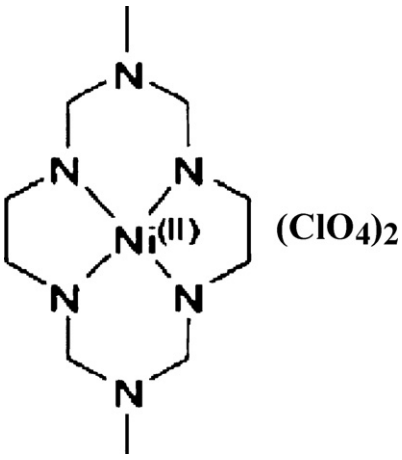

Fig. 1. Complex1 (1,8-dimethyl-1,3,6,8,10,13-hexaazacyclotetradecane), nickel(II) perchlorate.

were used. Ammonium acetate buffer (pH 4.5) was prepared as reported earlier [32].

2.2. Experimental procedure

Stock solutions of MG (0.97 g/L) and complex1 (8.3 mM) were prepared using double distilled water. Freshly prepared KPS solution was used for all experiments. These stock solutions were diluted to get solutions of desired concentrations. For all experiments, MG (10 mg/L), KPS (1 g/L) and complex1 (200 μM) were used unless otherwise specified. All reactions were carried out at 27 ± 2 °C at pH 7 unless specified. pH was adjusted to desired value with help of pH meter (EU Tech) by adding 0.1N H_2SO_4 or NaOH.

Decolourization of MG was monitored spectrophotometrically using JASCO V-570 UV/VIS/NIR. A reaction mixture of 2 mL was prepared by adding appropriate volumes of stock solutions of MG and KPS. KPS stock solution was added to MG and mixed thoroughly using a micropipette for 25 s, and then change in absorption spectrum was recorded at different time intervals. Similarly, for measuring change in absorbance in presence of complex1, reaction mixture (2 mL) contained complex1 in addition to MG and KPS.

Kinetics of degradation of MG was studied by monitoring decrease in absorbance at 618 nm every 10 s, after an initial delay of 25 s (time taken to mix the reactants thoroughly) [34]. This initial delay was maintained uniformly in all experiments. Change in absorbance at 618 nm was fitted to first order equation (mono-exponential decay) to obtain rate constants of decolourization of MG. Origin lab 6.1 software was used for all kinetic analysis.

Kinetic experiments were carried out with different concentrations of KPS and complex1, to investigate effect of initial concentration of KPS and complex1, respectively. Effect of pH on degradation of MG by KPS and KPS in presence of complex1 was studied at different pH (3, 7 and 9). Effect of Ni(II) and Fe(II) metal ions on degradation of MG by KPS was also studied at pH (3, 7 and 9). Effect of initial concentration of MG (10 mg/L and 30 mg/L) by KPS and KPS in presence of complex1 was studied using HPLC. In all spectrophotometric measurements, concentration of MG was maintained at 10 mg/L because concentration more than 10 mg/L caused saturation of absorbance.

2.3. HPLC analysis

Degradation of MG was studied by high-performance liquid chromatography (HPLC), using Shimadzu UFLC, equipped with

a phenomenex C18 HPLC column (250 mm × 4.5 mm, 5 μm) and SPDM 20A Prominence diode array detector. The measurement was performed with 20:80 (v/v) ammonium acetate buffer (pH 4.5)/acetonitrile as mobile phase in isocratic mode with flow rate of 1 mL/min. For each analysis, 100 μL of sample was injected and chromatogram was monitored at 618 nm.

2.4. Microbial assays

Microbial assays were performed according to standard literature procedures [35,36]. Sterile distilled water was used. Reaction mixture (1 mL) containing MG (20 mg/L), KPS (2 g/L) and complex1 (400 μM) was prepared by adding appropriate volumes of respective stock solutions. This solution was mixed thoroughly and kept undisturbed for 60 min. After 60 min, 1 mL of 2X NB was added to the above solution followed by addition of *E. coli* cells (~10^6). The contents were mixed well and incubated in a shaking incubator for overnight at 37 °C. Similar procedure was followed for control experiment except that reaction mixture contained only 1 mL MG (20 mg/L). 0.1 mL of above culture suspensions were spread plated on nutrient agar plates followed by overnight incubation at 37 °C. Above microbial assay consisted of two replicates.

2.5. TOC analysis

TOC was measured using Shimadzu TOC-V_{CSH} analyser with a nondispersive infrared (NDIR) detector. For TOC analysis, an aliquot of 20 mL was taken at specific time intervals from reaction mixture (100 mL) containing appropriate concentration of MG, KPS and complex1 [27].

2.6. LC–ESI–MS analysis

LC–ESI–MS analysis was performed using Thermo Finnigan LCQ Deca LC/MS/MS Electrospray quadrupole ion trap mass spectrometer. Surveyor LC was equipped with a C-18 column (150 mm × 2 mm). The measurement was performed in acetonitrile/water = 60:40 (v/v) as mobile phase with flow rate of 0.3 mL/min and injection volume of 5 μL. MG solution and MG solution treated with KPS and complex1 for 1 h was injected for analysis. Nitrogen was used as sheath and auxiliary gas. Ion source conditions were; sheath gas flow rate ~7.5 L/min. Capillary temperature was maintained at 200 °C and capillary voltage was kept at 15 V. Ion-spray voltage and tube lens offset were maintained at +4.5 kV and −7 V respectively. Normalized collusion energy was varied from 30% to 60% for fragmentation profile, and other parameters were similar to earlier report [37].

3. Results and discussion

Absorption spectra of MG showed three main peaks with absorption maxima at 618, 425 and 315 nm (Fig. 2a). Absorbance of these bands decreased upon addition of KPS to MG with a significant decrease in absorbance at 618 nm, and became almost zero at ~60 min (Fig. 2a). At 60 min, a new weak peak with absorption maximum around 365 nm was observed. These spectral changes revealed the ability of KPS to degrade MG. Earlier, disappearance of absorption band (500–700 nm) with peak at 618 nm was monitored to study degradation of MG by various methods [30–32].

HPLC chromatogram of MG monitored at 618 nm showed a single sharp peak with retention time (RT) at 4 min, which corresponds to MG (Fig. 2b) [32]. A very weak peak was also detected at RT 3.5 min, which could be due to trace impurities. Addition of KPS to MG resulted in decrease of intensity of these peaks, and formation of new peak with RT at 1.8 min (Fig. 2b). MG

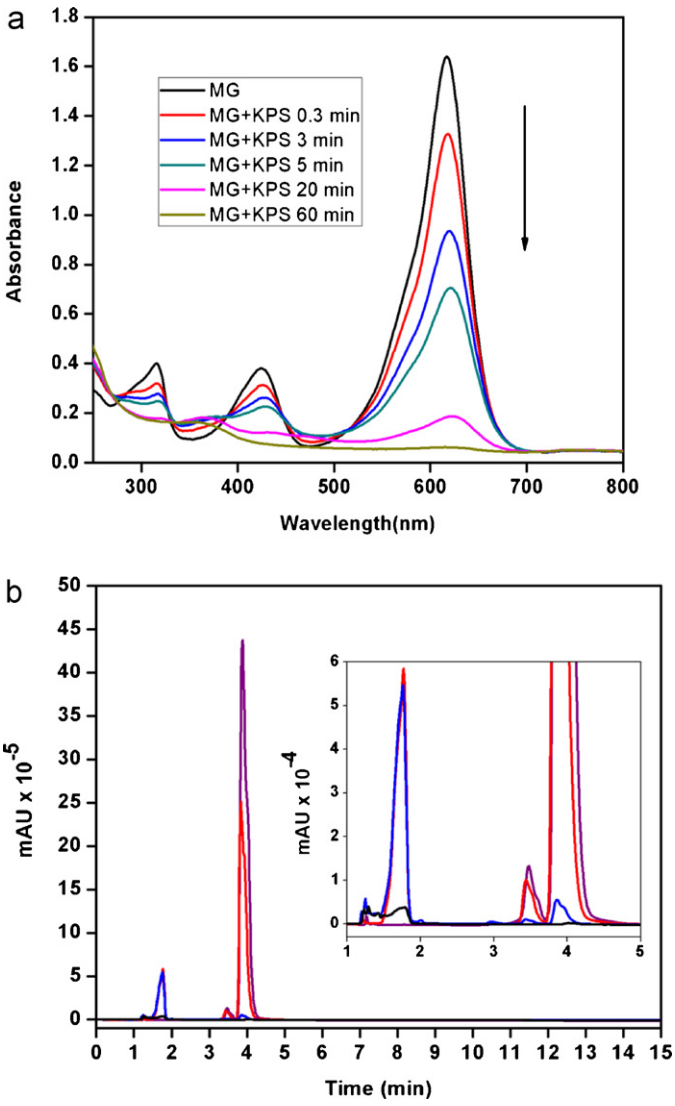

Fig. 2. (A) Absorption spectrum of MG (10 mg/L) after addition of KPS (1 g/L) at different time intervals. (B) HPLC chromatogram (618 nm) of MG (10 mg/L) after addition of KPS (1 g/L) at different time intervals. Colours: Violet – only MG, Red – 5 min, Blue – 20 min, Black – 60 min. (For interpretation of the references to colour in this figure legend, the reader is referred to the web version of this article.)

peak at 4 min completely disappeared after 60 min, while peak at RT 1.8 min was reduced to negligible level (Fig. 2b, inset). HPLC results clearly showed that KPS has ability to decompose MG to other species, leading to degradation. Earlier, it has been reported that peak at 1.8 min correspond to N-demethylated MG species, which are known to have absorbance around 594, 608 and 618 nm [32].

Absorption spectral changes of MG observed after addition of both KPS and complex1 showed a rapid decrease in absorption at 618 nm within 20 min (Fig. 3a). Moreover, after 60 min, a shoulder around 450 nm and also a peak around 290 nm were observed (Fig. 3b), which corresponds to trivalent nickel species formed due to reaction between KPS and complex1, as reported earlier [25]. The corresponding HPLC profiles monitored at 618 nm also revealed that MG, as well as, N-demethylated species with absorption around 618 nm were degraded within 20 min on addition of KPS with complex1 (Fig. 3b). Interestingly, rate of degradation of MG by KPS increased nine times higher in presence of complex1 than rate of degradation of MG by KPS alone (Table 1 and Fig. 4).

Table 1
Rate constants determined for degradation of MG by KPS under various conditions.

Reaction	KPS (g/L)	Complex1 (μM)	pH	Rate constants (min^{-1})
MG + KPS	1	–	7	0.11 ± 0.01
MG + KPS	1	–	3	0.20 ± 0.01
MG + KPS	1	–	9	0.23 ± 0.02
MG + KPS	1.5	–	7	0.14 ± 0.01
MG + KPS	2	–	7	0.19 ± 0.02
MG + KPS + complex1	1	200	7	0.93 ± 0.05
MG + KPS + complex1	1	200	3	0.59 ± 0.02
MG + KPS + complex1	1	200	9	0.63 ± 0.03
MG + KPS + complex1	1	50	7	0.71 ± 0.03
MG + KPS + complex1	1	10	7	0.25 ± 0.01
MG + KPS + Ni(II)[a]	1	–	7	0.12 ± 0.01
MG + KPS + Ni(II)[a]	1	–	3	0.14 ± 0.01
MG + KPS + Ni(II)[a]	1	–	9	0.11 ± 0.01
MG + KPS + Fe(II)[a]	1	–	3, 7, 9	Not determined[b]

Initial MG concentration for the above reactions is 10 mg/L.
[a] 200 μM.
[b] Reaction incomplete.

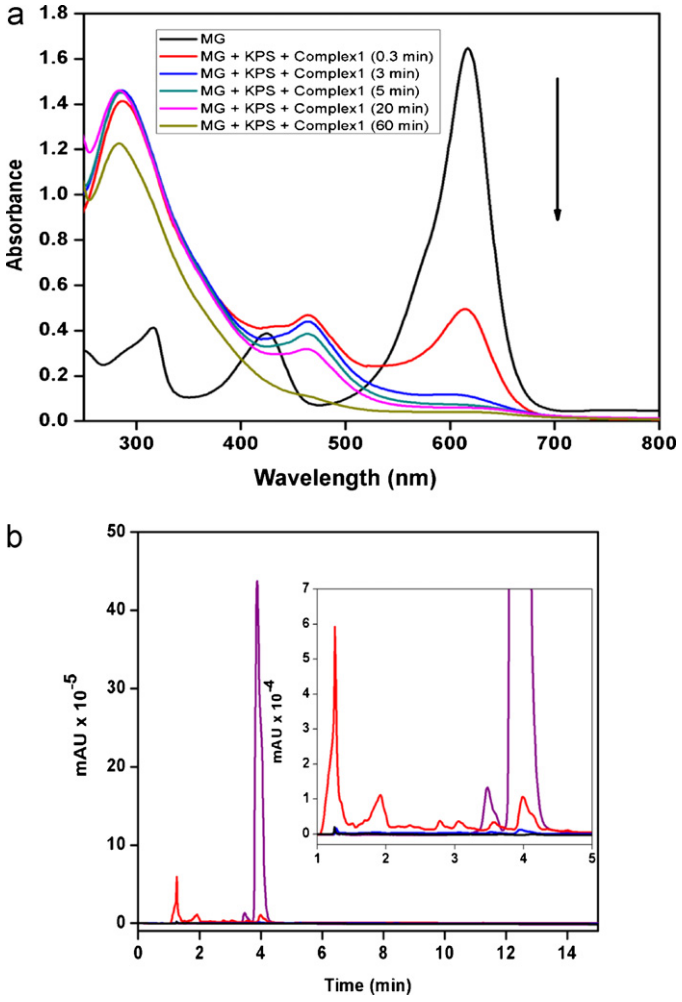

Fig. 3. (A) Absorption spectrum of MG (10 mg/L) after addition of KPS in presence of complex1 at different time intervals. (B) HPLC chromatogram (618 nm) of MG (10 mg/L) after addition of KPS in presence of complex1 (200 μM) at different time intervals. Colours: Violet – only MG, Red – 5 min, Blue – 20 min, Black – 60 min. (For interpretation of the references to colour in this figure legend, the reader is referred to the web version of this article.)

3.1. Effect of initial concentration of KPS and complex1

Rate of degradation of MG was found to increase on increasing concentration of KPS (Table 1 and Fig. 5a). On increasing the concentration of KPS, more reactive radicals could be generated and rate of MG degradation could become faster. Similar trend was observed for photochemical oxidation of Arsenic using persulphate [38].

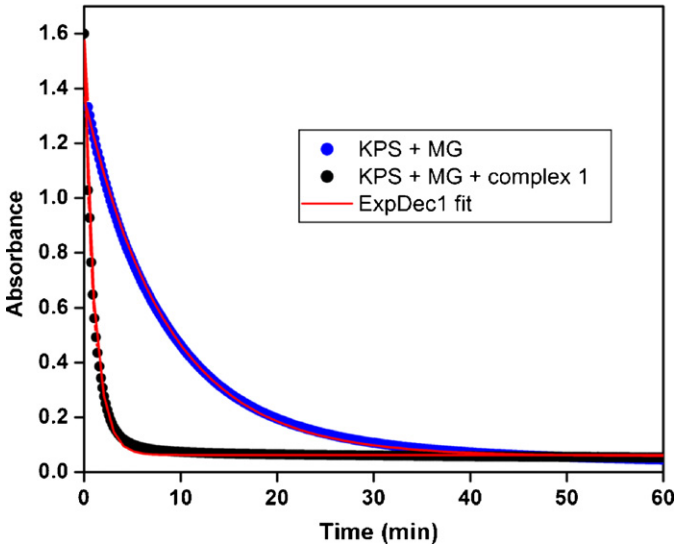

Fig. 4. Degradation of MG (10 mg/L) by KPS (1 g/L) in presence and absence of complex1 (200 μM) ExpDec1 fit (mono exponential decay).

Rate of degradation of MG by KPS in presence of complex1 (50–200 μM) was not significantly changed (Table 1 and Fig. 5b). However, on decreasing concentration of complex1 to as low as 10 μM, rate constant was decreased approximately four times. These results indicated that an optimum concentration of complex1 was required for effective decomposition of KPS and generation of reactive radicals for degradation of MG.

3.2. Effect of pH

Rates of degradation of MG at pH 3 and 9 were found to be almost similar, and slightly higher than at pH 7 (Table 1 and Fig. 6a). It is known that decomposition of KPS is enhanced by acid catalysis [39]. Moreover, base such as sodium hydroxide is also known to activate decomposition of persulphate [16]. Increase in rate of degradation of MG by KPS at pH 3 and 9 in present study was due to acid catalysis and base activation of KPS, respectively.

Rapid redox reaction between KPS and complex1 generates reactive sulphate radicals as well as trivalent nickel species, which

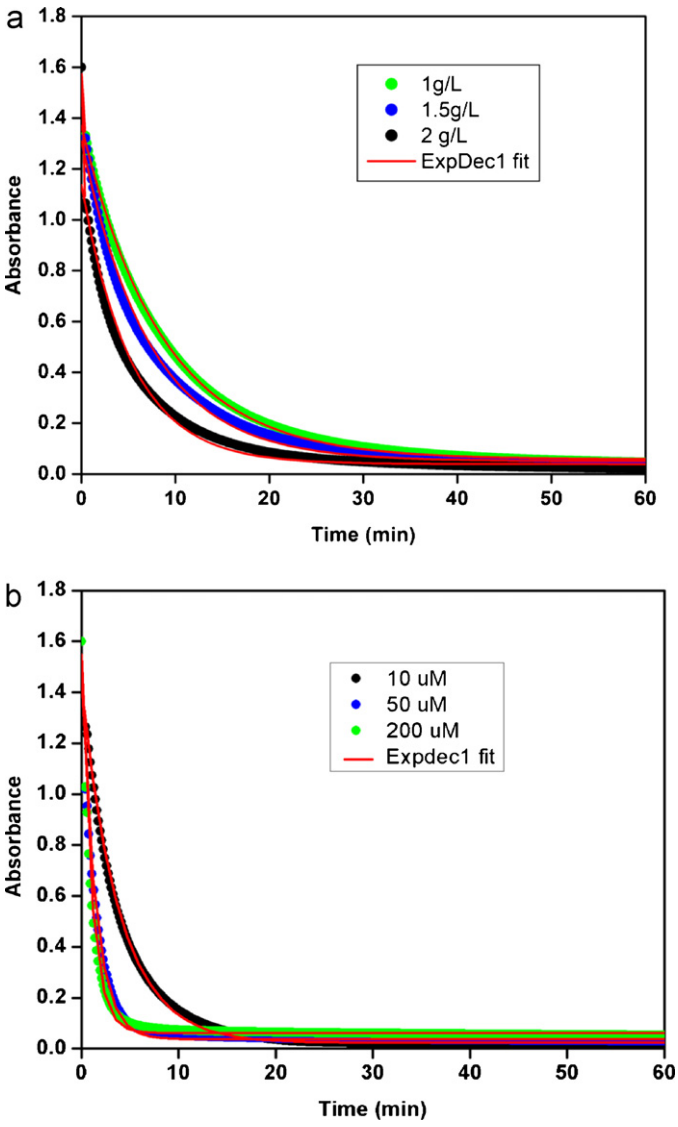

Fig. 5. (A) Degradation of MG (10 mg/L) with different concentrations of KPS. (B) Degradation of MG (10 mg/L) by KPS (1 g/L) in presence of different concentrations of complex1.

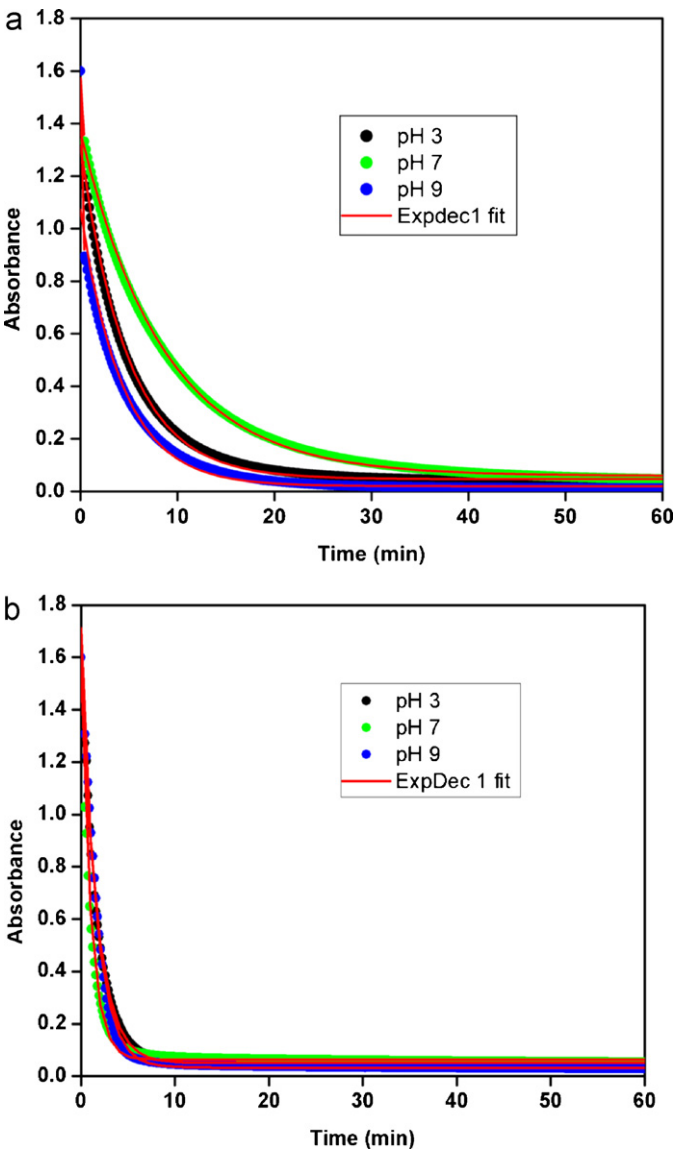

Fig. 6. (A) Degradation of MG (10 mg/L) by KPS (1 g/L) at various pH values. (B) Degradation of MG (10 mg/L) by KPS (1 g/L) in presence of complex1 (200 μM) at various pH values.

were reported to be strong oxidizing agents [25,26]. Therefore, degradation of MG by KPS became rapid in presence of complex1. Present results also show that degradation of MG by complex1-activated KPS was faster and more efficient than KPS activated by acid catalysis or base.

Rates of degradation of MG by KPS in presence of complex1 at pH 3 and 9 were found to be almost similar, and slightly lower at pH 7 (Table 1 and Fig. 6b). Earlier, it has been suggested that trivalent nickel species act as effective catalyst for oxidation process in aqueous neutral media and slightly alkaline media than under acidic condition, and the present results are in accordance with these reports [26]. Moreover, stability of trivalent nickel species is dependent on pH, nature of ligands and type of axial coordinating ions [26,39,40]. It is known that stability of trivalent species is highest in acidic, lowest in alkaline and intermediate in neutral conditions [26,40,41], indicating that trivalent nickel species are highly stabilized under acidic conditions and not favourable for oxidation reactions. It is important to note that, although there was a variation in rate of degradation of MG by KPS in presence of complex1 at pH range 3–9, advantage of KPS – complex1 mediated degradation of MG is that, MG is degraded effectively over a broad range of pH.

3.3. Effect of initial concentration of MG

HPLC chromatogram obtained for degradation of MG (30 mg/L) by KPS after 60 min of treatment showed peaks with RT at 1.8 and 4 min, which corresponds to N-demethylated species and MG, respectively (Fig. 7). However, HPLC chromatogram obtained for degradation of MG (10 mg/L) by KPS after 60 min of treatment showed that peak at RT 1.8 min was very weak and peak at RT 4 min almost disappeared. Thus, the results showed that as initial concentration of dye was increased, efficiency of degradation of MG, as well as N-demethylated species by KPS (1 g/L) was reduced. Similar trend was also observed for degradation of MG on increasing initial concentration of MG from 10 mg/L to 30 mg/L, by KPS in presence of complex1 (Fig. 7). Degradation of MG by KPS is associated with concentration of reactive radicals in solution. On increasing the initial dye concentration, degradation became incomplete due to less availability of reactive radicals in solution [38]. However, overall degradation of MG (10 mg/L and 30 mg/L) by KPS is more effective in presence of complex1 than by KPS alone.

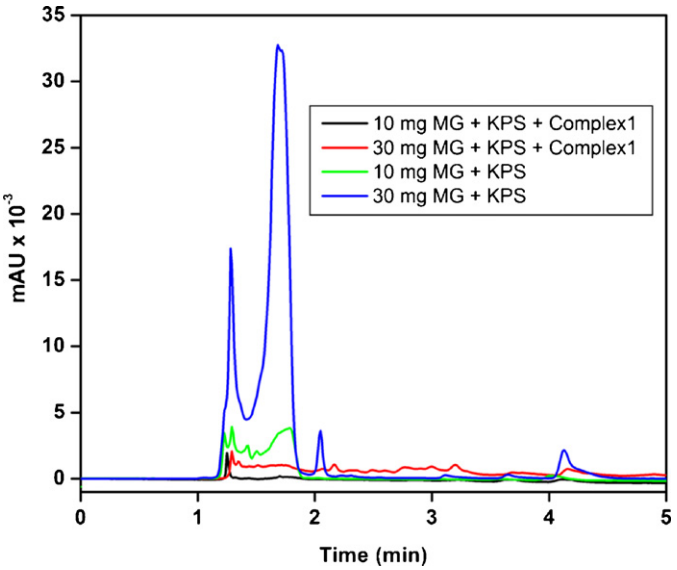

Fig. 7. HPLC chromatogram (618 nm) of MG (10 mg/L and 30 mg/L) after addition of KPS (1 g/L) in absence and presence of complex1 (200 μM).

3.4. Effect of nickel(II) and iron(II) ions

Rate of degradation of MG by KPS in presence of Ni(II) (200 μM) at pH 3–9 was similar to rate of degradation of MG by KPS alone (Table 1). On the other hand, degradation of MG by KPS in presence Fe(II) (200 μM) at pH 3–9 showed relatively higher absorbance at 618 nm (Fig. 8a), indicating that degradation was not efficient. Moreover, HPLC chromatogram showed a peak at 4 min corresponding to MG, and peaks at 1.8 min and 3.5 corresponding to N-demethylated species produced during degradation (Fig. 8b) [32]. These results clearly showed that, in presence of Fe(II), both MG and N-demethylated species are not effectively degraded compared to degradation of MG by KPS in presence of complex1.

On the basis of decrease in absorption at 618 nm and disappearance of MG peak with RT at 4 min in LC chromatogram, order of degradation of MG under mentioned experimental conditions is as follows:

KPS: ferrous sulphate < KPS: nickel chloride < KPS < KPS: complex1

Effect of various parameters observed for degradation of MG by KPS and by KPS in presence of complex1 followed a similar trend as observed for degradation of MG by Fenton processes [30] and Ozonation [27]. However, it is important to note that present results showed that degradation of MG by KPS and by KPS in presence of complex1 was effective over a wide pH range (3–9) while Fenton processes as well as Ozonation process were mainly effective under acidic conditions.

3.5. Total organic carbon analysis

TOC analysis results showed that treatment of MG (20 mg/L) with KPS (2 g/L) alone could reduce 7% of TOC whereas treatment of MG (20 mg/L) with KPS (2 g/L) along with complex1 (400 μM) could remove 11% of TOC within 3 h (Fig. 9). This shows that treatment of MG with KPS alone and KPS with complex1 not only results in degradation of MG but also in reduction of TOC.

3.6. Antimicrobial activity of MG before and after degradation

E. coli cells suspended in NB containing MG (untreated) were incubated overnight, and solution was found to be clear (Fig. 10a). This solution when spread plated on NB agar and incubated

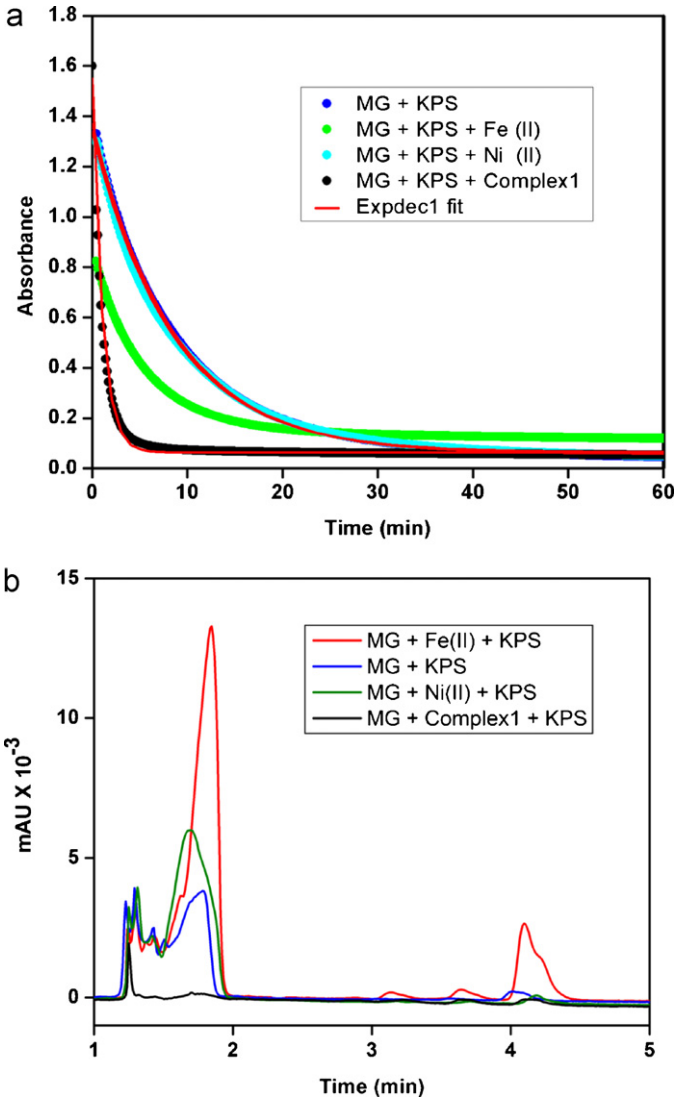

Fig. 8. (A) Degradation of MG (10 mg/L) by KPS (1 g/L) in absence and presence of complex1 (200 μM); Fe (II) (200 μM) and Ni(II) (200 μM). (B) HPLC chromatogram of MG (10 mg/L) after addition of KPS in absence and presence of complex1 (200 μM); Fe (II) (200 μM) and Ni(II) (200 μM) after 60 min.

overnight, did not show formation of any bacterial colonies (Fig. 10b), which clearly revealed that MG alone is toxic to bacteria. On the other hand, when *E. coli* cells were suspended in NB, containing degraded MG (after treatment with KPS in presence of complex1 for 60 min), solution was found to be turbid (Fig. 10c). This solution when spread plated and observed after overnight incubation, displayed formation of numerous bacterial colonies (matt growth) (Fig. 10d). Similarly, control experiments which were carried out in absence of MG also showed matt growth (Fig. 10e and f). Thus, above results indicated that KPS and complex1 system has propensity to reduce antibacterial activity of MG drastically under *in vitro* conditions. Earlier, it has been shown that degradation of MG by ozonation processes [27] and decolourization of MG by dye-decolourizing bacterium (*Shewanella decolorationis* NTOU1) [42] showed reduction in antibacterial activity.

3.7. Mass spectral analysis of MG and its degradation intermediates

MG solution showed a single peak in TIC plot, and its corresponding mass spectrum had a clear peak with 329 *m/z* (S.I. Fig. 1).

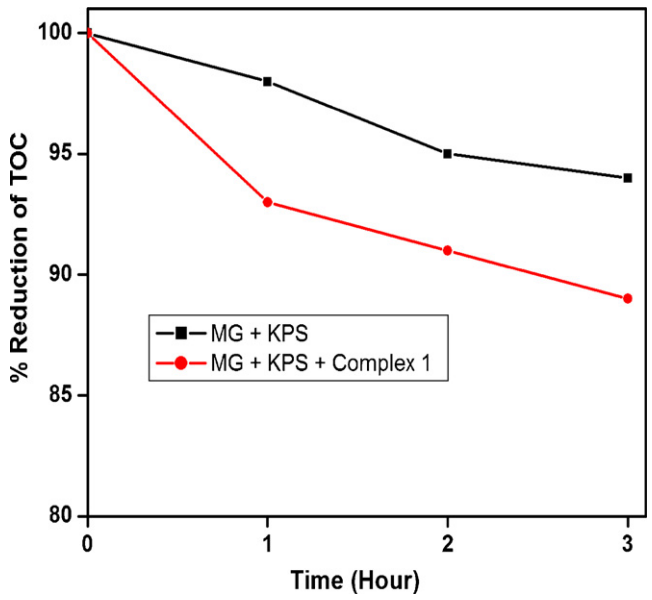

Fig. 9. TOC reduction (%) of MG (20 mg/L) after the treatment with KPS (2 g/L) in absence and presence of complex1 (400 μM).

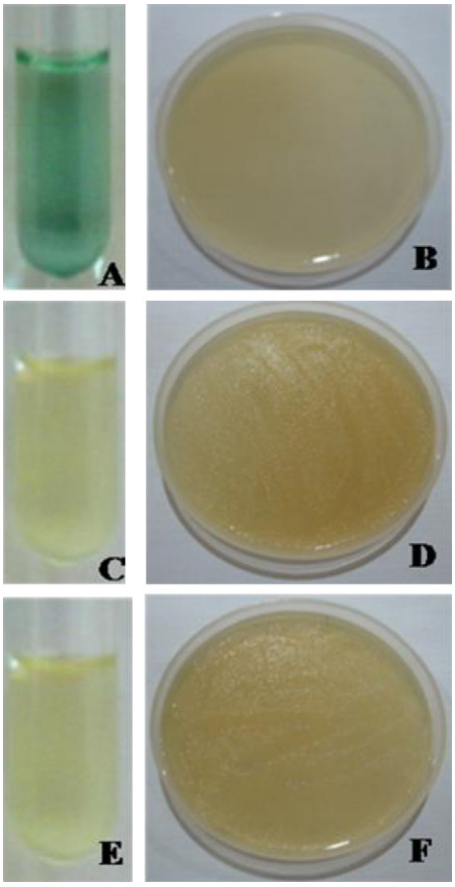

Fig. 10. Photograph showing effect of MG (10 mg/L) on growth of *E. coli* (~10^6 cells) before and after treatment by KPS (1 g/L) and complex1 (200 μM). A, C and E tubes containing *E. coli* with MG, *E. coli* with MG after treatment by KPS and complex1, and *E. coli*., respectively. B, D and F are the plates corresponding to the tubes A, C and E respectively after overnight incubation.

Table 2
m/*z* values of degradation intermediates and tentative structures.

TIC peak[a]	Tentative structure		*m*/*z*
A	MG–3CH_2	A_1	287.16
A	DLBP + OH	A_2	242.11
A	DLBP–CH_2 + OH	A_3	228.50
A	DLBP + 2OH	A_4	257.11
A	BPA + HSO_4^-	A_5	266.00
A	BPA + CH_3 + OH	A_6	200.10
A	MG–4CH_2–NH + 4OH	A_7	322.11
B	MG–2CH_2–NH + 4OH	B_1	352.15
B	MG–4CH_2 + 2OH	B_2	305.13
C	LMG	C_1	331.00
C	MG–4CH_2–2NH + 4OH	C_2	309.10
C	MG–2CH_2–NH	C_3	286.16

[a] Peaks and their corresponding RT: A (1.48–1.53 min), B (2.38–2.41 min) and C (3.61–3.65 min).

Degraded MG solution showed 3 peaks (A, B, C) in TIC plot (S.I. Fig. 2), and corresponding mass spectra of these peaks revealed the formation of a variety of degraded intermediates, and complexity of degradation.

Earlier studies on degradation of MG mediated by hydroxyl radicals reported the formation of complex reaction mixture with N-demethylated intermediates of MG, DLBP (dimethylaminobenzophenone) and their hydroxyl adducts along with many other possible intermediates [32,43,44]. Analysis of present mass spectral results clearly showed ions that could correspond to N-demethylated intermediates, hydroxyl adducts of N-demethylated intermediates and DLBP (Table 2). Interestingly, these results showed that persulphate mediated degradation of MG could form hydroxyl adducts.

It is known that in aqueous solution sulphate radicals react with water to produce hydroxyl radicals that could react with aromatic ring to form hydroxyl adducts [45,46]. Moreover, sulphate radicals could directly attack the aromatic ring and form hydroxyl adducts [46,47]. Thus, in the present study, formation of hydroxyl adducts of degradation intermediates could be attributed to both the sulphate radicals and secondary hydroxyl radicals generated upon activation of KPS by complex1.

ESI-MS/MS analysis of MG showed following ions, 329.17 (MG); 285.12 (MG–2CH_2–NH_2); 251.20 (MG–C_6H_6); 237.11 (MG–C_6H_6–CH_2) and 208.28 (MG–C_6H_6–CH_2), which was similar to earlier report (S.I. Fig. 3) [32]. Importantly, ESI-MS/MS of degradation intermediate A_3 (DLBP–CH_2 + OH) with 228.5 *m*/*z* value showed a fragment ion with 149.10 *m*/*z* (A_3–C_6H_6); (S.I. Fig. 3). Similar fragmentation has been reported for bezenophenone type molecule [48]. Thus, this result further supports the presence of degradation intermediate with hydroxyl adduct.

Hydroxyl radicals could cause deamination of aromatic amines [43,44,52,53]. Earlier, report on the oxidation of MG by persulphate suggested the formation of biphenyl amine (BPA) intermediates [34]. In addition, persulphate is known to react with aromatic amines to form aromatic amine sulphate adducts [49–51]. A peak with 266 *m*/*z* identified in the mass spectra could correspond to BPA sulphate adduct (A_5) (S.I. Fig. 2). ESI-MS/MS of this intermediate A_5 (BPA + HSO_4^-), showed a fragment ion with 169.2 *m*/*z* (A_5–H_2SO_4). (S.I. Fig. 3). In addition, intermediate A_6 (BPA + CH_3 + OH) with 200.19 *m*/*z* showed following fragment ions; 122.5 (A_6–C_6H_6), 144.25 (A_6–CH_2–C–NH–CH_3). Earlier similar fragmentations were observed for aromatic amino derivatives [54–56] (S.I. Fig. 3).

As mentioned above, reactive sulphate and hydroxyl radicals could generate a variety of intermediates, however, identification of all intermediates by mass spectrometry was not possible. It is important to note that, several factors such as concentration of intermediates present in analysis solution and the amount obtained after separation in the solid phase column, HPLC

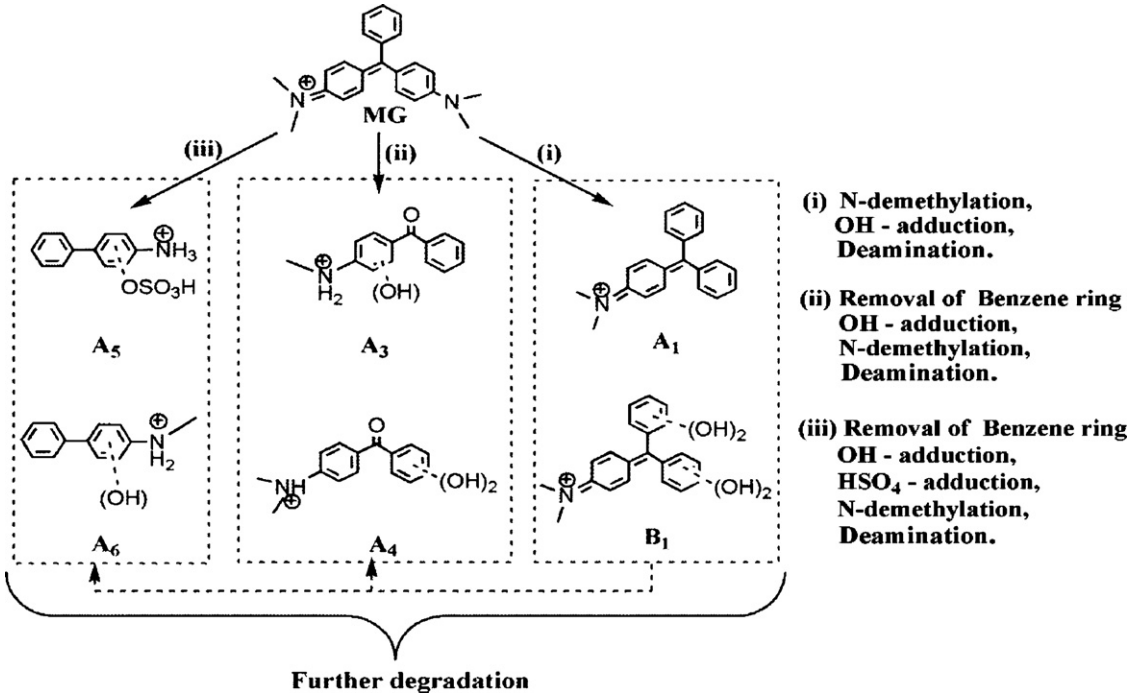

Scheme 1. Possible reactions in degradation of MG by KPS in presence of complex1.

separation protocols, type of molecules and stability of charged ions, mass spectrometer used, presence of a variety of compounds and alkali metal ions in sample, complexity due to fragmentations in ESI source, and others could affect the analysis by mass spectrometer [32,37,43,44].

Based on above discussion and available literature, important possible reactions for degradation of MG by KPS and complex1 are proposed (Scheme 1). Proposed degradation mechanism includes major reactions such as N-demethylation, hydroxyl adduct formation and removal of benzene ring, as reported earlier [32,43,44].

4. Conclusions

MG and its structurally related N-demethylated species were almost completely degraded by KPS alone. Interestingly, degradation of MG by KPS and complex1 oxidation system was found to occur in wide pH range (3–9) with enhanced rate as compared to KPS alone. Degradation of MG by KPS in trace amount of Fe(II) ions was incomplete whereas addition of trace amount of Ni(II) ions had no significant effect on degradation of MG by KPS. Degradation of MG by KPS was dependent on initial concentration of KPS, complex1, and MG. Microbial assay revealed removal of antibacterial activity of MG after treatment of MG by KPS in presence of complex1, indicating that this oxidation system has ability to decrease toxicity of MG significantly towards bacteria. Moreover, TOC analysis indicated the ability of KPS, and KPS in presence of complex1 to reduce TOC. Hydroxyl adducts of MG, DLBP and BPA intermediates were identified in degraded solution by LC–ESI–MS analysis. Thus, this study demonstrates that KPS and complex1 oxidation system could be a better choice for degradation of environmentally persistent and hazardous MG and possibly other related dyes that are released in to water bodies.

Acknowledgements

H.P. acknowledges research Grant No. BT/PR133316/GBP/27/251/2009 from Department of Biotechnology (DBT), Government of India. G.S. and P.P. acknowledge DBT and Council of Scientific and Industrial Research (CSIR) for fellowships, respectively. Authors are thankful to Dr. Meenal Kowshik, BITS, Pilani, Goa for providing bacterial culture, Prof. Shyamalava Mazumdar and Mr. Shibdas Banerjee, TIFR, Mumbai for ESI–MS, Director and Chairperson, Syngenta India Ltd., Goa for TOC analysis. IMA facility of BITS-Pilani, Goa, India, is acknowledged.

Appendix A. Supplementary data

Supplementary data associated with this article can be found, in the online version, at doi:10.1016/j.jhazmat.2012.01.031.

References

[1] S.J. Culp, F.A. Beland, Malachite green: a toxicological review, Int. J. Toxicol. 15 (1996) 219–238.
[2] C.F. Chang, C.H. Yang, Y.O. Shu, T.I. Chen, M.S. Shu, I.C. Liao, Effects of temperature, salinity and chemical drugs on the in vitro propagation of the Dinoflagellate parasite, *Amylodinium ocellatum*, Asian Fish Soc. P31 (2001).
[3] S. Srivastava, R. Sinha, D. Roy, Toxicological effects of Malachite green, Aquat. Toxicol. 66 (2004) 319–329.
[4] A. Stammati, C. Nebbia, I.D. Angelis, A.G. Albo, M. Carletti, C. Rebecchi, F. Zampaglioni, M. Dacasto, Effects of Malachite green (MG) and its major metabolite, leucomalachite green (LMG), in two human cell lines, Toxicol. In Vitro 19 (2005) 853–858.
[5] T. Sauer, G. Cesconeto Neto, H.J. José, R.F.P.M. Moreira, Kinetics of photocatalytic degradation of reactive dyes in a TiO_2 slurry reactor, J. Photochem. Photobiol. A 149 (2002) 147–154.
[6] N. Daneshvar, D. Salari, A.R. Khataee, Photocatalytic degradation of azo dye acid red 14 in water: investigation of the effect of operational parameters, J. Photochem. Photobiol. A 157 (2003) 111–116.
[7] C.-Y. Chen, J.-T. Kuo, C.-Y. Cheng, Y.-T. Huang, I.H. Ho, Y.-C. Chung, Biological decolorization of dye solution containing Malachite green by *Pandoraea pulmonicola* YC32 using a batch and continuous system, J. Hazard. Mater. 172 (2009) 1439–1445.
[8] A. Romero, A. Santos, F. Vicente, C. González, Diuron abatement using activated persulphate: Effect of pH, Fe(II) and oxidant dosage, Chem. Eng. J. 162 (2010) 257–265.
[9] M.I. Stephen, N.H. Ince, J.R. Bolton, UV/H_2O_2 degradation and toxicity reduction of textile azo dyes, J. Adv. Oxid. Technol. 2 (1997) 442–448.
[10] D.T. Gonenc, N.H. Ince, Treatability of a textile azo dye by UV/H_2O_2, Environ. Technol. 18 (1997) 179–185.
[11] M.P. Georgiou, D.A. Aivasidis, K. Gimouhopoulos, Degradation of azo-reactive dyes by ultraviolet radiation in the presence of hydrogen peroxide, Dyes Pigments 52 (2002) 69–78.

[12] A. Mohey El-Dein, J.A. Libra, U. Wiesmann, Mechanism and kinetic model for the decolorization of the azo dye Reactive Black 5 by hydrogen peroxide and UV radiation, Chemosphere 52 (2003) 1069–1077.
[13] R.J. Watts, A.L. Teel, Treatment of contaminated soils and groundwater using ISCO, Pract. Period. Hazard. Radioact. Toxicol. Waste Manage. 10 (2006) 2–9.
[14] C. Liang, C.J. Bruell, Thermally activated persulfate oxidation of trichloroethylene: experimental investigation of reaction orders, Ind. Eng. Chem. Res. 47 (2008) 2912–2918.
[15] W.K. Wilmarth, A. Haim, Mechanisms of oxidation by peroxydisulfate ion, in: J.O. Edwards (Ed.), Peroxide Reaction Mechanisms, Interscience, New York, 1962, pp. 175–225.
[16] O.S. Furman, A.L. Teel, R.J. Watts, Mechanism of base activation of persulfate, Environ. Sci. Technol. 44 (2010) 6423–6428.
[17] G.P. Anipsitakis, D.D. Dionysiou, Radical generation by the interaction of transition metals with common oxidants, Environ. Sci. Technol. 38 (2004) 3705–3712.
[18] R.H. Waldemer, P.G. Tratnyek, R.L. Johnson, J.T. Nurmi, Oxidation of chlorinated ethenes by heat-activated persulfate: kinetics and products, Environ. Sci. Technol. 41 (2007) 1010–1015.
[19] X. Liang, P.J. Sadler, Cyclam complexes and their applications in medicine, Chem. Soc. Rev. 33 (2004) 246–266.
[20] K.P. Wainwright, Synthetic and structural aspects of the chemistry of saturated polyaza macrocyclic ligands bearing pendant coordinating groups attached to nitrogen, Coord. Chem. Rev. 166 (1997) 35–90.
[21] A. McAuley, S. Subramanian, Synthesis, spectroscopy, and redox behavior of the binuclear complex cation $[Ni_2(6,6'\text{-spirobi(cyclam)})]^{4+}$ (cyclam = 1,4,8,11-tetraazacyclotetradecane): characteristics of a transient Ni(II)–Ni(III) species, Inorg. Chem. 36 (1997) 5376–5383.
[22] I. Zilbermann, E. Maimon, H. Cohen, D. Meyerstein, Redox chemistry of nickel complexes in aqueous solutions, Chem. Rev. 105 (2005) 2609–2626.
[23] K. Nag, A. Chakravorty, Monovalent, trivalent and tetravalent nickel, Coord. Chem. Rev. 33 (1980) 87.
[24] E. Zeigerson, I. Bar, J. Bernstein, L.J. Kirschenbaum, D. Meyerstein, Stabilization of the tervalent nickel complex with meso-5,7,7,12,14,14-hexamethyl-1,4,8,11-tetraazacyclotetradecane by axial coordination of anions in aqueous solution, Inorg. Chem. 21 (1982) 73–80.
[25] R.I. Haines, J.E. Rowley, Structure and kinetics of oxidation of amphiphilic nickel(II) pentaazamacrocycles by peroxodisulfate and by a nickel(III) pendant-arm macrocycle, J. Incl. Phenom. Macrocycl. 47 (2003) 25–32.
[26] I. Zilbermann, A. Meshulam, H. Cohen, D. Meyerstein, Stabilization of nickel(III)-1,8-dimethyl-1,3,6,8,10,13-hexaazacyclotetradecane by axial binding of anions in neutral aqueous solutions, Inorg. Chim. Acta 206 (1993) 127–130.
[27] E. Kusvuran, O. Gulnaz, A. Samil, Ö. Yildirim, Decolorization of malachite green, decolorization kinetics and stoichiometry of ozone-malachite green and removal of antibacterial activity with ozonation processes, J. Hazard. Mater. 186 (2011) 133–143.
[28] A.G.S. Prado, L.L. Costa, Photocatalytic decouloration of malachite green dye by application of TiO_2 nanotubes, J. Hazard. Mater. 169 (2009) 297–301.
[29] Y. Liu, Y. Ohko, R. Zhang, Y. Yang, Z. Zhang, Degradation of malachite green on Pd/WO_3 photocatalysts under simulated solar light, J. Hazard. Mater. 184 (2010) 386–391.
[30] B.H. Hameed, T.W. Lee, Degradation of malachite green in aqueous solution by Fenton process, J. Hazard. Mater. 164 (2009) 468–472.
[31] N. Modirshahla, M.A. Behnajady, Photooxidative degradation of Malachite Green (MG) by UV/H_2O_2: influence of operational parameters and kinetic modeling, Dyes Pigments 70 (2006) 54–59.
[32] Y. Ju, S. Yang, Y. Ding, C. Sun, A. Zhang, L. Wang, Microwave-assisted rapid photocatalytic degradation of Malachite green in TiO_2 suspensions: mechanism and pathways, J. Phys. Chem. A 112 (2008) 11172–11177.
[33] M.P. Suh, S.G. Kang, Synthesis and properties of nickel(I1) and copper(I1) complexes of 14-membered hexaaza macrocycles, 1,bdimethyl- and 1,8-diethyl-1,3,6,8,10,13-hexaazacyclotetradecane, Inorg. Chem. 27 (1988) 2544–2546.
[34] T. Mushinga, S.B. Jonnalagadda, A kinetic approach for the mechanism of malachite green-peroxydisulphate reaction in aqueous solution, Int. J. Chem. Kinet. 24 (1992) 41–49.
[35] V. Lorian, Antibiotics in Laboratory Medicine, 2005.
[36] S. Egger, R.P. Lehmann, M.J. Height, M.J. Loessner, M. Schuppler, Antimicrobial properties of a novel silver-silica nanocomposite material, Appl. Environ. Microbiol. 75 (2009) 2973–2976.
[37] S. Banerjee, H. Prakash, S. Mazumdar, Evidence of molecular fragmentation inside the charged droplets produced by electrospray process, J. Am. Soc. Mass Spectrom. 22 (2011) 1707–1717.
[38] B. Nepollian, E. Celik, H. Choi, Photochemical oxidation of arsenic(III) to arsenic(V) using peroxydisulfate ions as an oxidizing agent, Environ. Sci. Technol. 42 (2008) 6179–6184.
[39] I.M. Kolthoff, I.K. Millar, The chemistry of persulfate. I. The kinetics and mechanism of the decomposition of the persulfate ion in aqueous medium, J. Am. Chem. Soc. 73 (7) (1951) 3055–3059.
[40] E. Zeigerson, I. Bar, J. Bernstein, L.J. Kirschenbaum, D. Meyerstein, Stabilization of the tervalent nickel complex with *meso*-5,7,7,12,14,14-hexamethyl-1,4,8,11-tetraazacyclotetradecane by axial coordination of anions in aqueous solution, Inorg. Chem. 21 (1982) 73–80.
[41] I. Zilbermann, E. Maimon, H. Cohen, D. Meyerstein, Redox chemistry of nickel complexes in aqueous solutions, Chem. Rev. 105 (2005) 2609–2625.
[42] C.H. Chen, C.F. Chang, S.M. Liu, Partial degradation mechanisms of malachite green and methyl violet B by *Shewanella decolorationis* NTOU1 under anaerobic conditions, J. Hazard. Mater. 177 (2010) 281–289.
[43] Y. Ju, S. Yang, Y. Ding, C. Sun, C. Gu, Z. He, C. Qin, H. He, B. Xu, Microwave-enhanced H_2O_2-based process for treating aqueous malachite green solutions: intermediates and degradation mechanism, J. Hazard. Mater. 171 (2009) 123–132.
[44] L.A. Perez-Estrada, A. Aguera, M.D. Hernando, S. Malato, A.R. Fernandez-Alba, Photodegradation of malachite green under sunlight irradiation: kinetics and toxicity of the transformation products, Chemosphere 70 (2008) 2068–2075.
[45] H. Hori, A. Yamamoto, E. Hayakawa, S. Taniyasu, N. Yamashita, S. Kutsuna, Efficient decomposition of environmentally persistent trefluorocarcoxylic acids by use of persulfate as a photochemical oxidant, Environ. Sci. Technol. 39 (2005) 2383–2388.
[46] X.-Y. Yu, Z.C. Bao, J.R. Barker, Free radical reactions involving $Cl^{\bullet}$, $Cl_2^{\bullet-}$ and $SO_4^{\bullet-}$ in the 248 nm photolysis of aqueous solutions containing $S_2O_8^{2-}$ and Cl^-, J. Phys. Chem. A 108 (2004) 295–308.
[47] G.P. Anipsitakis, D.D. Dionysiou, M.A. Gonzalez, Cobalt-mediated activation of peroxomonosulfate and sulfate radical attack on phenolic compounds. implication of chloride ions, Environ. Sci. Technol. 40 (2006) 1000–1007.
[48] N. Negreira, I. Rodriguez, M. Ramil, E. Rubi, R. Cela, Solid-phase extraction followed by liquid chromatography–tandem mass spectrometry for the determination of hydroxylated benzophenone UV absorbers in environmental water samples, Anal. Chim. Acta 654 (2009) 162–170.
[49] E.J. Behrman, The ortho-para ratio and the intermediate in the persulfate oxidation of aromatic amines (the Boyland-Sims Oxidation), J. Org. Chem. 57 (1992) 2266–2270.
[50] E.J. Behrman, Studies on the reaction between peroxydisulfate ions and aromatic amines. The Boyland-Sims Oxidation, JACS 89 (1967) 2424–2428.
[51] E. Boyland, D. Manson, P. Sims, D.C. Willams, The resistance of some o-aminoaryl sulphates to hydrolysis by aryl sulphatases, Biochem. J. 62 (1956) 68–71.
[52] P. Neta, R.W. Fessenden, Hydroxyl radical reactions with phenols and anilines as studied by electron spin resonance, J. Phys. Chem. 78 (1974) 523–529.
[53] G.N.R. Tripathi, Q. Sun, Time-resolved Raman study of the oxidation mechanism of aromatic diamines by $^{\bullet}OH$ radical in water, J. Phys. Chem. A 103 (1999) 9055–9060.
[54] M. Villagrasa, M. Guillamon, A. Navarro, E. Eljarrat, D. Barcelo, Development of a pressurized liquid extraction solid-phase extraction followed by liquid chromatography–electrospray ionization tandem mass spectrometry method for the quantitative determination of benzoxazolinones and their degradation products in agricultural soil, J. Chromatogr. A 1179 (2008) 190–197.
[55] R.J. Turesky, J.P. Freeman, R.D. Holland, D.M. Nestorick, D.W. Miller, D.L. Ratnasinghe, F.F. Kadlubar, Identification of aminobiphenyl derivatives in commercial hair dyes, Chem. Res. Toxicol. 16 (2003) 1162–1173.
[56] S.T. Wu, K. Cao, S.J. Bonacorsi, H. Zang, M. Jemal, Distinguishing a phosphate ester prodrug from its isobaric sulphate metabolite by mass spectrometry with the metabolite standard, Rapid Commun. Mass Spectrom. 23 (2009) 3107–3113.